Transmission dynamics of Zika virus in island populations: a modelling analysis of the 2013–14 French Polynesia outbreak

Adam J. Kucharski[1,*], Sebastian Funk[1], Rosalind M. Eggo[1], Henri-Pierre Mallet[2], W. John Edmunds[1], Eric J. Nilles[3]

1 Centre for the Mathematical Modelling of Infectious Diseases, London School of Hygiene & Tropical Medicine, London, United Kingdom
2 Bureau de Veille Sanitaire, Direction de la Santé, Polynésie française
3 World Health Organization, Suva, Fiji

*E-mail: adam.kucharski@lshtm.ac.uk

Abstract

Between October 2013 and April 2014, more than 30,000 cases of Zika virus (ZIKV) disease were reported in French Polynesia. ZIKV has also been reported in Africa and Asia, and in 2015 the virus spread to South America and the Caribbean. Infection with ZIKV has been associated with neurological complications including Guillain-Barré Syndrome (GBS) and microcephaly, which led the World Health Organization declare a Public Health Emergency of International Concern in February 2015. To better understand the transmission dynamics of ZIKV, we used a mathematical model to examine the 2013–14 outbreak on the six major archipelagos of French Polynesia. Our median estimates for the basic reproduction number ranged from 1.9–3.1, with an estimated 11.2% (95% CI: 10.1-12.9%) of total infections reported. As a result, we estimated that 86% (95% CI: 75-93%) of the total population of the six archipelagos were infected during the outbreak. There were 42 GBS cases reported during the ZIKV outbreak in French Polynesia, but the presence of a large number of unreported ZIKV infections could have implications for the design of case-control studies to further investigate a possible association between the two. Based on the demography of French Polynesia, our results also imply that if ZIKV infection provides complete protection against future infection, it would take 15–20 years before there are a sufficient number of susceptible individuals for ZIKV to re-emerge, which is on the same timescale as the circulation of dengue virus serotypes in the region. Our analysis suggests that ZIKV may exhibit similar dynamics to dengue virus in island populations, with transmission characterised by large, sporadic outbreaks with a high proportion of asymptomatic or unreported cases.

Introduction

Originally identified in Africa [1], the first large reported outbreak of Zika virus (ZIKV) disease occurred in Yap during April–July 2007 [2], followed by an outbreak in French Polynesia between October 2013 and April 2014 [3], and cases in other Pacific countries [4,5]. During 2015, local transmission was also reported in South American countries, including Brazil [6,7] and Colombia [8].

Transmission of ZIKV is predominately vector-borne, but can also occur via sexual contact and blood transfusions [9]. The virus is spread by the *Aedes* species of mosquito [10], which is also the vector for dengue virus (DENV), ZIKV is therefore likely to be capable of sustained transmission in other tropical areas [11]. As well as causing symptoms such as fever and rash, ZIKV infection has also been linked to increased incidence of neurological sequelae, including Guillain-Barré Syndrome (GBS) [12,13] and microcephaly in infants born to mothers who were infected with ZIKV during pregnancy [14]. On 1st February 2015, the World Health Organization declared a Public Health Emergency of International Concern in response to the clusters of microcephaly and other neurological disorders reported in Brazil, possibly linked to the recent rise in ZIKV incidence. The same phenomena were observed in French Polynesia, with 42 GBS cases [13] reported during the outbreak. In addition to the GBS cluster, there were 18 fetal or newborn cases with unusual and severe neurological features reported between March 2014 and May 2015 in French Polynesia, including 10 cases with microcephaly and severe brain lesions, and 8 normocephalic cases with severe anatomical or functional neurological abnormalities [15].

Given the potential for ZIKV to spread globally, it is crucial to characterise the transmission dynamics of the infection. This includes estimates of key epidemiological parameters, such as the basic reproduction number, R_0 (defined as the average number of secondary cases generated by a typical infectious individual in a fully susceptible

population), and of how many individuals (including both symptomatic and asymptomatic) are typically infected during an outbreak. Such estimates could help assist with outbreak planning, assessment of potential countermeasures, and the design of studies to investigate putative associations between ZIKV infection and other conditions.

Islands can be useful case studies for outbreak analysis. Small, centralised populations are less likely to sustain endemic transmission than a large, heterogeneous population [16], which means outbreaks are typically self-limiting after introduction from external sources [17]. Further, if individuals are immunologically naive to a particular pathogen, it is not necessary to consider potential effect of pre-existing immunity on transmission dynamics [18]. Using a mathematical model of vector-borne infection, we examined the transmission dynamics of ZIKV on six archipelagos in French Polynesia during the 2013–14 outbreak. We inferred the basic reproduction number, and the overall size of the outbreak, and hence how many individuals would still be susceptible to infection in coming years.

Methods

Data

We used weekly reported numbers of suspected ZIKV infections from the six main regions of French Polynesia between 11th October 2013 and 28th March 2014 (Table 1), taken from Centre d'hygiène et de salubrité publique situation reports [19, 20]. Confirmed and suspected cases were reported from sentinel surveillance sites across the country; the number of sentinel sites varied in number from 27–55 during the outbreak. In total, 8,744 suspected cases were reported from the sentinel sites. As there were 162 healthcare sites across all six regions, it has been estimated that around 30,000 suspected cases attended health facilities in total [19]. For each region, we calculated the proportion of total sites that acted as sentinels, to allow us to adjust for variation in reporting over time in the analysis. Population size data were taken from the 2012 French Polynesia Census [21]. In our analysis, the first week with at least one reported case was used as the first observation date.

Table 1. Geographical breakdown of the 2013–14 French Polynesia ZIKV outbreak.

Regions	Population	Suspected cases	PCR confirmed cases
Tahiti	178,100	4,966	128
Iles sous-le-vent	33,100	1,131	166
Moorea	16,200	440	22
Tuamotu-Gambier	15,800	612	9
Marquises	8,600	455	21
Australes	6,800	733	36

Mathematical model

We used a compartmental mathematical model to simulate vector-borne transmission [22]. Both people and mosquitoes were modelled using a susceptible-exposed-infectious-removed (SEIR) framework. This model incorporated delays as a result of the intrinsic (human) and extrinsic (vector) latent periods (Figure 1). Since there is evidence that asymptomatic DENV-infected individuals are

capable of transmitting DENV to mosquitoes [23], we assumed the same for ZIKV: all people in the model transmitted the same, regardless of whether they displayed symptoms or were reported as cases.
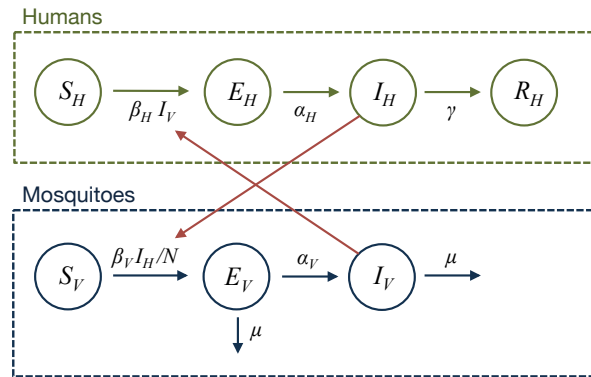

Figure 1. Human-vector transmission model schematic. S^H represents the number of susceptible people, E^H the number of latent people, I^H the number of infectious people, R^H the number recovered people that have recovered. Similarly, S^V represents the proportion of mosquitoes currently susceptible, E^V the proportion in their latent period, and I^V the proportion of mosquitoes infectious. β_V is the transmission rate from humans to mosquitoes; $1/\alpha_H$ and $1/\alpha_V$ are the mean latent periods for humans and mosquitoes respectively; $1/\gamma$ is the mean infectious period for humans; $1/\mu$ is the mean lifespan of mosquitoes; and N is the human the population size.

The main vectors for ZIKV in French Polynesia are thought to be *Ae. aegypti* and *Ae. polynesiensis* [12]. In the southern islands, the extrinsic incubation period for *Ae. polynesiensis* is longer during the cooler period from May to September [24], which may act to reduce transmission. However, climate data from French Polynesia [25] indicated that the ZIKV outbreaks on the six archipelagos ended before a decline in mean temperature or rainfall occurred (Figure S1). Hence it is likely that transmission ceased as a result of depletion of susceptible humans rather than seasonal changes in vector transmission. Therefore we did not include seasonal effects in our analysis.

In the model, S^H represents the number of susceptible people, E^H is the number of people currently in their latent period, I^H is the number of infectious people, R^H is the number of people that have recovered, C denotes the cumulative number of people infected (used to fit the model), and N is the population size. Similarly, S^V represents the proportion of mosquitoes currently susceptible, E^V the proportion in their latent period, and I^V the proportion of mosquitoes currently infectious. As the mean human lifespan is much longer than the outbreak duration, we omitted human births and

deaths. The full model is as follows:

$$dS^H/dt = -\beta_H S_t^H I_t^V \tag{1}$$

$$dE^H/dt = \beta_H S_t^H I_t^V - \alpha E_t^H \tag{2}$$

$$dI^H/dt = \alpha_H E_t^H - \gamma I_t^H \tag{3}$$

$$dR^H/dt = \gamma I_t^H \tag{4}$$

$$dC/dt = \alpha_H E_t^H \tag{5}$$

$$dS^V/dt = -\beta_V \frac{I_t^H}{N} - \delta S_t^V \tag{6}$$

$$dE^V/dt = \beta_V \frac{I_t^H}{N} - (\delta + \alpha_V) E_t^V \tag{7}$$

$$dI^V/dt = \alpha_V E_t^V - \delta I_t^V \tag{8}$$

Parameter definitions and values are given in Table 2. We used informative prior distributions for the human latent period, α_H, because the incubation period in humans is typically between 2–7 days [26,27]; the infectious period, $1/\gamma$, lasted for 4–7 days in clinical descriptions of 297 PCR-confirmed cases in French Polynesia [20]; and the the extrinsic latent period, which has been estimated at $1/\alpha_v$=10 days [1]. We assumed uniform prior distributions for all other parameters.

Table 2. Parameters used in the model. Prior distributions are given for all parameters, along with source(s) if the prior incorporates a specific mean value. All rates are given in units of days^{-1}.

Parameter	Definition	Prior	Source
$1/\alpha_V$	extrinsic latent period	Gamma(μ=10.5, σ=1)	[1]
$1/\alpha_H$	intrinsic latent period	Gamma(μ=4, σ=1)	[26,27]
$1/\gamma$	human infectious period	Gamma(μ=5, σ=1)	[20]
$1/\delta$	mosquito lifespan	Gamma(μ=7.8, σ=1)	[24]
β_H	vector-to-human transmission rate	$\mathcal{U}(0,\infty)$	
β_V	human-to-vector transmission rate	$\mathcal{U}(0,\infty)$	
r	proportion of cases reported	$\mathcal{U}(0,1)$	
ϕ	reporting dispersion	$\mathcal{U}(0,\infty)$	

Serological analysis of samples from blood donors between July 2011 and October 2013 suggests that only 0.8% of the population of French Polynesia were seropositive to ZIKV [28]; we therefore assumed that the population was fully susceptible initially. We also assumed that the initial number of latent and infectious people were equal (i.e. $E_0^H = I_0^H$), and the same for mosquitoes ($E_0^V = I_0^V$). The basic reproduction number is equal to the product of the average number of mosquitoes infected by the typical infectious human, and vice versa:

$$R_0 = \frac{\beta_V}{\gamma} \times \frac{\alpha_V}{\delta + \alpha_V} \frac{\beta_H}{\mu} \ . \tag{9}$$

Statistical inference

Model fitting was performed using Markov chain Monte Carlo (MCMC). Incidence in week t, denoted c_t, was defined as the difference in the cumulative proportion of cases over the previous week i.e. $c_t = C(t) - C(t-1)$. We defined κ_t as the proportion of total sites that reported cases as sentinels in week t. To account for potential variability

in reporting, we assumed the number of confirmed and suspected cases in week t followed a negative binomial distribution with mean $r\kappa_t c_t$ and dispersion parameter ϕ [29]. The joint posterior distribution of the parameters was obtained from sampling 30,000 MCMC iterations, after a burn-in period of 10,000 iterations (Figures S2–S7). The model was implemented in R version 3.2.3 [30].

Demographic model

We implemented simple a demographic model to examine the repletion of the number of susceptible individuals over time. In 2014, French Polynesia had a birth rate of b=15.47 births/1,000 population, a death rate of d=4.93 deaths/1,000 population, and net migration rate of m=−0.87 migrants/1,000 [31]. The number of susceptible individuals in year t, $S(t)$, and total population size, $N(t)$, was therefore expressed as the following discrete process:

$$N(t) = N(t-1) + bN(t-1) - dN(t-1) - mN(t-1) \tag{10}$$
$$S(t) = S(t-1) + bN(t-1) - dS(t-1) - mS(t-1) \tag{11}$$

We set $S(2014)$ as the fraction of the population remaining in the S compartment at the end of the 2013–14 ZIKV outbreak, and propagated the model forward to estimate susceptibility in future years. The effective reproduction number, $R_{\text{eff}}(t)$, in year t was the product of the estimated basic reproduction number, and the proportion of the population susceptible: $R_{\text{eff}}(t) = R_0 S(t)$. We sampled 5,000 values from the estimated joint posterior distributions of $S(2014)$ and R_0 to obtain the curves shown in Figure 3.

Results

Across the six regions, the median estimates for the basic reproduction number, R_0, ranged from 1.9 (95% CI: 1.4–3.7) in Marquises to 3.1 (95% CI: 2.1–4.8) in Moorea (Table 3). The credible interval was broadest for the smallest region, Australes, for which we estimated R_0 2.9 (1.7–79). Our results suggest that only a small proportion of ZIKV infections were reported as suspected cases: our median estimates implied that between 8–22% of infections were reported. Estimated dispersion in reporting was greatest for Marquises and Australes (Figures S2–S7), reflecting the variability in the observed data (Figure 2), even after adjusting for variation in the number of sentinel sites.

The estimated proportion of the population that were infected during the outbreak (including both reported and unreported cases) was above 75% for all six regions (Table 3), and we estimated that 86% (95% CI: 75-93%) of the total population were infected during the outbreak. Serological analysis of the ZIKV outbreak on Yap also found a high level of infection, with 73% (95% CI 66–77%) of individuals aged 3 and over infected during the outbreak [2]. Our posterior estimates for the human latent and infectious periods were consistent with the assumed prior distributions (Figures S2–S7), suggesting either that there was no strong evidence that these parameters had a different distribution, or that the model had limited ability to identify these parameters from the available data.

During the 2013–14 outbreak in French Polynesia, there were 42 reported cases of GBS [13]. This corresponds to an incidence rate of 15.3 (95% binomial CI: 11.0–20.7) cases per 100,000 population, whereas the established annual rate for GBS is 1–2 cases per 100,000 [10]. In total, there were 8,744 confirmed and suspected ZIKV cases reported at sentinel sites in French Polynesia, which gives an incidence rate of 480 (95% CI: 346–648) GBS cases per 100,000 suspected Zika cases reported at these sites.
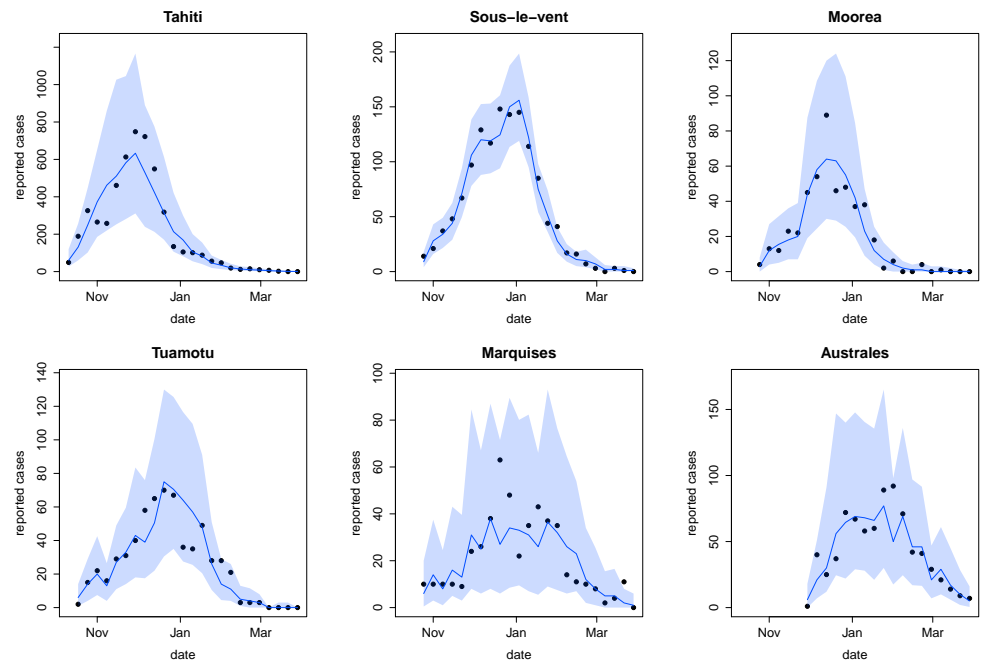
Figure 2. Comparison of reported cases and fitted model trajectories. Black dots show weekly reported confirmed and suspected ZIKV cases from sentinel sites. Blue line shows median of 2,000 simulated trajectories from the fitted model, adjusted for variation in reporting over time; shaded region shows 95% credible interval.

Table 3. Estimated parameters for ZIKV infection. Estimates for the basic reproduction number, R_0; the proportion of infected individuals that were reported as suspected cases at sentinel sites; and the total proportion of the population infected (including both symptomatic and asymptomatic cases). Median estimates are given, with 95% credible intervals in parentheses. The full posterior distributions are shown in Figures S2–S7.

Region	R_0	Reported (%)	Infected (%)
Tahiti	2.4 (1.6-3.5)	14 (11-18)	87 (67-96)
Sous-le-vent	2.7 (2.2-3.3)	12 (11-13)	89 (83-94)
Moorea	3.1 (2.1-4.8)	7.6 (6.2-9.6)	95 (83-99)
Tuamotu-Gambier	2.2 (1.6-3.9)	8.8 (7.2-11)	82 (67-93)
Marquises	1.9 (1.4-3.7)	14 (10-20)	76 (54-89)
Australes	2.9 (1.7-79)	22 (17-29)	82 (63-95)

However, if we calculate the GBS incidence rate per estimated total ZIKV cases, we obtain a rate of 18.3 (12.9-24.5). These credible intervals overlap substantially with the above incidence rate calculated with population size as the denominator, indicating that the two rates are not significantly different.

Using a demographic model we also estimated the potential for ZIKV to cause a future outbreak in French Polynesia. We combined our estimate of the proportion of the population that remained susceptible after the 2013–14 outbreak and R_0 with a birth-death-migration model to estimate the effective reproduction number, R_{eff}, of ZIKV in future years. If R_{eff} is greater than one, an epidemic would be possible in that location. Assuming that ZIKV infection confers lifelong immunity against infection with

129
130
131
132
133
134
135
136
137
138

ZIKV, our results suggest that it would likely take 15–20 years for the susceptible pool   139
in French Polynesia to be sufficiently replenished for another outbreak to occur   140
(Figure 3). This is remarkably similar to the characteristic dynamics of DENV in the   141
Pacific island countries and territories, with each of the four DENV serotypes   142
re-emerging in sequence every 15–20 years, likely as a result of the birth of a new   143
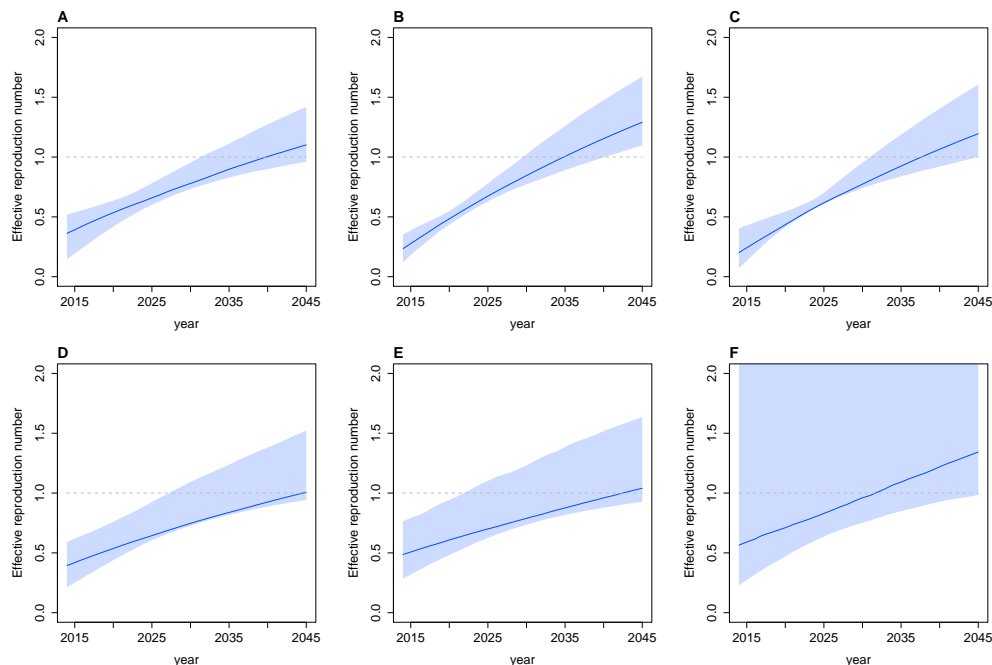generation of susceptible individuals [17,32].   144

Figure 3. Estimated growth in effective reproduction number as susceptible pool increases over time. (A) Tahiti, (B) Sous-le-vent, (C) Moorea, (D) Tuamotu, (E) Marquises, (F) Australes. Line shows median from 1,000 samples of the posterior distribution, shaded region shows 95% credible interval.

Discussion   145

Using a mathematical model of ZIKV transmission, we analysed the dynamics of the   146
infection during the 2013–14 outbreak in French Polynesia. In particular, we estimated   147
key epidemiological parameters, such as the basic reproduction number, R_0, and the   148
proportion of infections that were reported. Across the six regions, our median   149
estimates suggest that between 8–22% of infections were reported as suspected cases.   150
This does not necessarily mean these cases were asymptomatic; individuals may have   151
had mild symptoms and hence did not enter the healthcare system. For example,   152
although the attack rate for suspected ZIKV disease cases was 2.5% in the 2007 Yap   153
ZIKV outbreak, a household study following the outbreak found that around 19% of   154
individuals who were seropositive to ZIKV had experienced ZIKV disease-like symptoms   155
during the outbreak period [2].   156

Our median estimates for R_0 ranged from 1.9–3.1 across the six main archipelagos of   157
French Polynesia, and as a result the median estimates of the proportion of the   158
populations became infected in our model spanned 76–95%. The ZIKV outbreak in   159
French Polynesia coincided with a significant increase in Guillain-Barré syndrome (GBS)   160
incidence [13]. We found that although there was a raw incidence rate of 480 (95% CI: 161

346–648) GBS cases per 100,000 suspected ZIKV cases reported, the majority of the population was likely to have been infected during the outbreak, and therefore the rate per infected person was similar to the overall rate per capita. This could have implications for the design of case-control studies to test for an association between ZIKV infection and neurological complications.

If infection with ZIKV confers lifelong immunity, we found it would take at least a decade before re-invasion were possible. In the Pacific island countries and territories, replacement of DENV serotypes occurs every 4–5 years [17, 32], and therefore each specific serotype re-emerges in a 15–20 year cycle. The similarity of this timescale to our results suggest that ZIKV may exhibit very similar dynamics to DENV in island populations, causing infrequent, explosive outbreaks with a high proportion of the population becoming infected. However, it remains unclear whether ZIKV could become established as an endemic disease in larger populations, as dengue has.

For immunising infectious diseases, there is typically a 'critical community size', below which random effects frequently lead to disease extinction, and endemic transmission cannot be sustained [16]. Analysis of dengue outbreaks in Peru from 1994–2006 found that in populations of more than 500,000 people, dengue was reported in at least 70% of weekly records [33]. Large cities could have the potential to sustain other arboviruses too, and understanding which factors–from population to climate–influence whether ZIKV transmission can become endemic will be an important topic for future research. We did not consider seasonal variation in transmission as a result of climate factors in our analysis, because all six outbreaks ended before there was a substantial seasonal change in rainfall or temperature. If the outbreaks had ended as a result of seasonality, rather than depletion of susceptibles, it would reduce the estimated proportion of the population infected, and shorten the time interval before ZIKV would be expected to re-emerge.

There are some additional limitations to our analysis. We used a homogeneous mixing model, in which all individuals had equal chance of contact. In reality, there may be spatial heterogeneity in transmission, leading to a depletion of the susceptible human pool in some areas but not in others. As we were only fitting to a single time series for each region, we also assumed prior distributions for the latent and infectious periods in humans. If seroprevalence data become available in the future, they could give an indication of how many people were actually infected, which would make it possible to constrain more of the model parameters. However, such studies may require careful interpretation, as antibodies may cross-react between different flaviviruses [12].

Our results suggest that ZIKV transmission in island populations may follow similar patterns to dengue fever, generating large, sporadic outbreaks with a high degree of under-reporting. If a substantial proportion of such populations become infected during an outbreak, it may take several years for the infection to re-emerge in the same location. A high level of infection, combined with rare outbreaks, could also make it more challenging to establish a causal link between infection and concurrent neurological complications.

References

1. Hayes EB. Zika virus outside Africa. Emerging infectious diseases. 2009;15(9):1347.

2. Duffy MR, Chen TH, Hancock WT, Powers AM, Kool JL, Lanciotti RS, et al. Zika virus outbreak on Yap Island, federated states of Micronesia. New England Journal of Medicine. 2009;360(24):2536–2543.

3. Cao-Lormeau VM, Roche C, Teissier A, Robin E, Berry AL, Mallet HP, et al. Zika virus, French polynesia, South pacific, 2013. Emerging infectious diseases. 2014;20(6):1085.

4. Musso D, Cao-Lormeau VM, Gubler DJ. Zika virus: following the path of dengue and chikungunya? The Lancet. 2015;386(9990):243–244.

5. Roth A, Mercier A, Lepers C, Hoy D, Duituturaga S, Benyon E, et al. Concurrent outbreaks of dengue, chikungunya and Zika virus infections–an unprecedented epidemic wave of mosquito-borne viruses in the Pacific 2012–2014. Euro Surveill. 2014;19(1).

6. Campos GS, Bandeira AC, Sardi SI. Zika virus outbreak, Bahia, Brazil. Emerging infectious diseases. 2015;21(10):1885.

7. Corsica F. Zika virus transmission from French Polynesia to Brazil. Emerg Infect Dis. 2015;.

8. Camacho E, Paternina-Gomez M, Blanco PJ, Osorio JE, Aliota MT. Detection of Autochthonous Zika Virus Transmission in Sincelejo, Colombia. Emerg Infect Dis. 2016;22(5).

9. Musso D, Roche C, Robin E, Nhan T, Teissier A, Cao-Lormeau VM. Potential Sexual Transmission of Zika Virus. Emerging infectious diseases. 2015;21(2):359.

10. Musso D, Nilles EJ, Cao-Lormeau VM. Rapid spread of emerging Zika virus in the Pacific area. Clinical Microbiology and Infection. 2014;20(10):O595–O596.

11. Bogoch II, Brady OJ, Kraemer MU, German M, Creatore MI, Kulkarni MA, et al. Anticipating the international spread of Zika virus from Brazil. The Lancet. 2016;.

12. Oehler E, Watrin L, Larre P, Leparc-Goffart I, Lastere S, Valour F, et al. Zika virus infection complicated by Guillain-Barré syndrome-case report, French Polynesia, December 2013. Euro Surveill. 2014;19:20720.

13. Oehler E, Fournier E, Leparc-Goffart I, Larre P, Cubizolle S, Sookhareea C, et al. Increase in cases of Guillain-Barré syndrome during a Chikungunya outbreak, French Polynesia, 2014 to 2015. Euro surveillance: bulletin Europe en sur les maladies transmissibles= European communicable disease bulletin. 2015;20(48).

14. Schuler-Faccini L. Possible Association Between Zika Virus Infection and Microcephaly Brazil, 2015. MMWR Morbidity and Mortality Weekly Report. 2016;65.

15. Centre d'hygiène et de salubrité publique. Note sur les investigations autour des malformations cérébrales congénitales ayant suivi l'épidémie de zika de 2013-2014. December 2015;Available from: http://www.hygiene-publique.gov.pf/IMG/pdf/note_malformations_congenitales_cerebrales.pdf.

16. Keeling M, Grenfell B. Disease extinction and community size: modeling the persistence of measles. Science. 1997;275(5296):65.

17. Cao-Lormeau VM, Roche C, Musso D, Mallet HP, Dalipanda T, Dofai A, et al. Dengue virus type 3, South Pacific Islands, 2013. Emerging infectious diseases. 2014;20(6):1034.

18. Camacho A, Ballesteros S, Graham AL, Carrat F, Ratmann O, Cazelles B. Explaining rapid reinfections in multiple-wave influenza outbreaks: Tristan da Cunha 1971 epidemic as a case study. Proc Biol Sci. 2011 Apr;.

19. Centre d'hygiène et de salubrité publique. Surveillance de la dengue et du zika en Polynèsie française. 2014 March 28;Available from: `http://www.hygiene-publique.gov.pf/IMG/pdf/bulletin_dengue_28-03-14.pdf`.

20. Mallet HP, Vial AL, Musso D. Bilan de l'épidémie a virus ZIKA en Polynésie Francaise 2013–2014. Bulletin d'Information Sanitaires, Epidemiologiques et Statistiques. 2015;Available from: `http://www.hygiene-publique.gov.pf/IMG/pdf/no13_-_mai_2015_-_zika.pdf`.

21. Institut national de la statistique et des études économiques. Population des subdivisions administratives de Polynésie française. 2012;Available from: `http://www.insee.fr`.

22. Pandey A, Mubayi A, Medlock J. Comparing vector–host and SIR models for dengue transmission. Mathematical biosciences. 2013;246(2):252–259.

23. Duong V, Lambrechts L, Paul RE, Ly S, Lay RS, Long KC, et al. Asymptomatic humans transmit dengue virus to mosquitoes. Proc Natl Acad Sci U S A. 2015 Nov;112(47):14688–93.

24. Lardeux F, Cheffort J. Ambient temperature effects on the extrinsic incubation period of Wuchereria bancrofti in Aedes polynesiensis: implications for filariasis transmission dynamics and distribution in French Polynesia. Med Vet Entomol. 2001;15(2):167–76.

25. The World Bank. Climate Change Knowledge Portal. 2016;Available from: `http://sdwebx.worldbank.org/climateportal/index.cfm`.

26. Bearcroft W. Zika virus infection experimentally induced in a human volunteer. Transactions of the Royal Society of Tropical Medicine and Hygiene. 1956;50(5):438–441.

27. World Health Organisation, Western Pacific Region. Zika virus. 2016;Available from: `http://www.wpro.who.int/mediacentre/factsheets/fs_05182015_zika/en/`.

28. Aubry M, Finke J, Teissier A, Roche C, Broult J, Paulous S, et al. Seroprevalence of arboviruses among blood donors in French Polynesia, 2011–2013. International Journal of Infectious Diseases. 2015;41:11–12.

29. Bretó C, He D, Ionides EL, King AA. Time series analysis via mechanistic models. The Annals of Applied Statistics. 2009;p. 319–348.

30. R Core Team. R: A Language and Environment for Statistical Computing. 2015;Available from: `https://www.r-project.org/`.

31. CIA. The World Factbook. 2016;Available from: `https://www.cia.gov/library/publications/the-world-factbook/`.

32. Li Ds, Liu W, Guigon A, Mostyn C, Grant R, Aaskov J. Rapid displacement of dengue virus type 1 by type 4, Pacific region, 2007-2009. Emerg Infect Dis. 2010 Jan;16(1):123–5.

33. Chowell G, Torre C, Munayco-Escate C, Suarez-Ognio L, Lopez-Cruz R, Hyman J, et al. Spatial and temporal dynamics of dengue fever in Peru: 1994–2006. Epidemiology and infection. 2008;136(12):1667–1677.
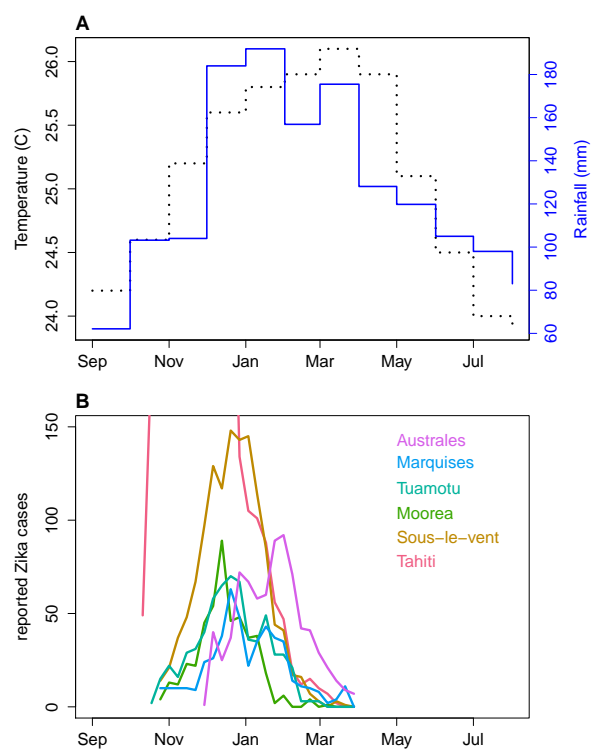
Supporting Information

Figure S1. Temporal change in climate and reported Zika incidence.
(A) Mean monthly temperature and rainfall in French Polynesia from 1990–2012. (B)
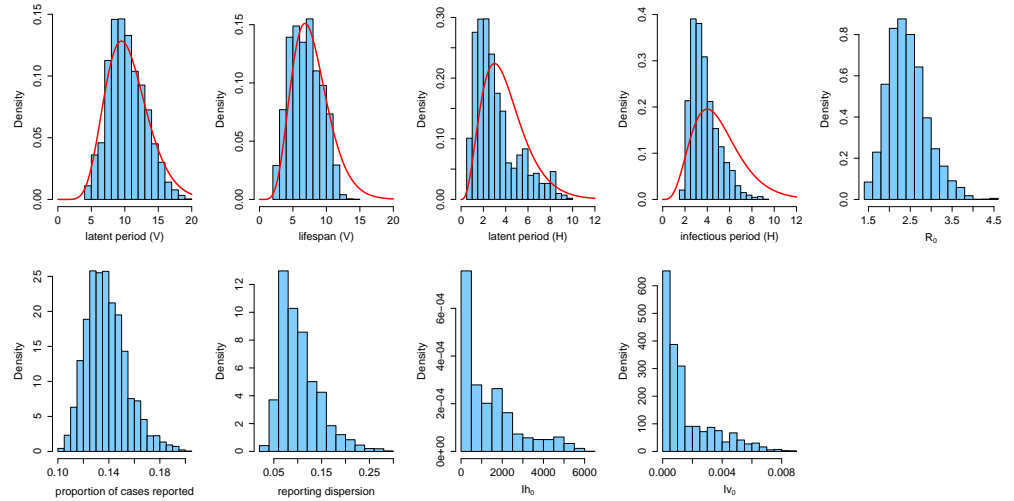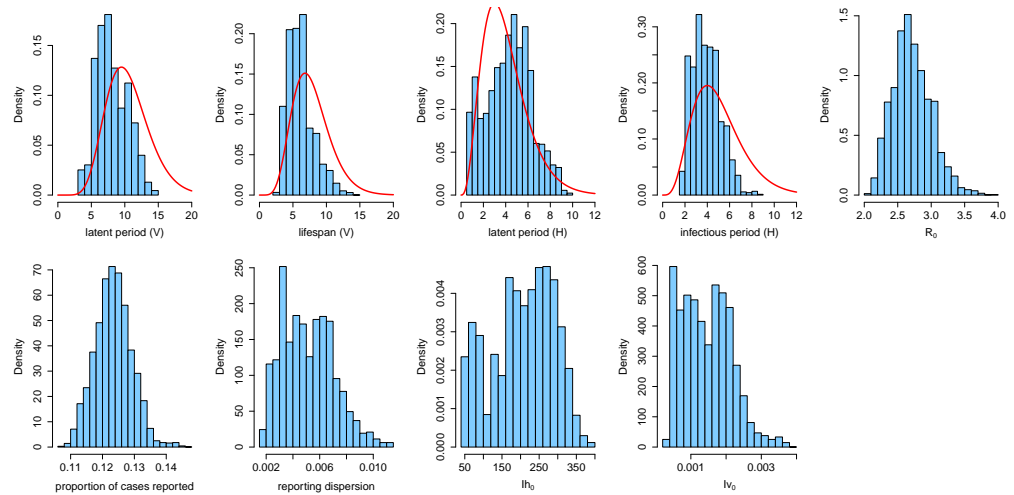Suspected ZIKV cases in 2013–14.

Figure S2. Posterior estimates for Tahiti.
Plot shows marginal posterior estimates for: the mean vector latent period and lifespan; the mean human latent and infectious periods; the basic reproduction number, R_0; the proportion of cases reported, r; the magnitude of environmental noise, ϕ; the number of initially infectious humans, and the proportion of the mosquito population initially infectious. Red lines show the assumed prior distributions for the latent periods in humans and mosquitoes, infectious period in humans, and mosquito lifespan.
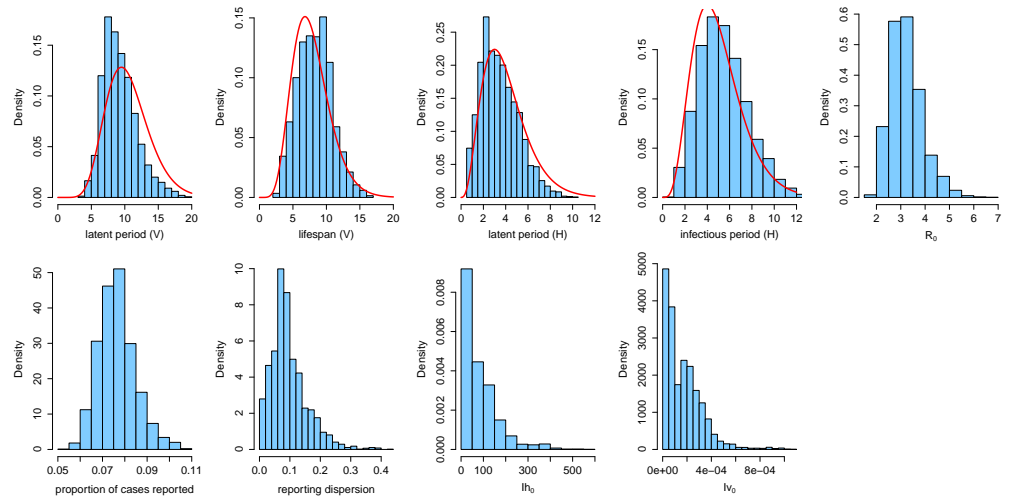

Figure S3. Posterior estimates for Iles sous-le-vent.
Plot shows marginal posterior estimates for: the mean vector latent period and lifespan; the mean human latent and infectious periods; the basic reproduction number, R_0; the proportion of cases reported, r; the magnitude of environmental noise, ϕ; the number of initially infectious humans, and the proportion of the mosquito population initially infectious. Red lines show the assumed prior distributions for the latent periods in humans and mosquitoes, infectious period in humans, and mosquito lifespan.

Figure S4. Posterior estimates for Moorea.
Plot shows marginal posterior estimates for: the mean vector latent period and lifespan; the mean human latent and infectious periods; the basic reproduction number, R_0; the proportion of cases reported, r; the magnitude of environmental noise, ϕ; the number of initially infectious humans, and the proportion of the mosquito population initially infectious. Red lines show the assumed prior distributions for the latent periods in humans and mosquitoes, infectious period in humans, and mosquito lifespan.
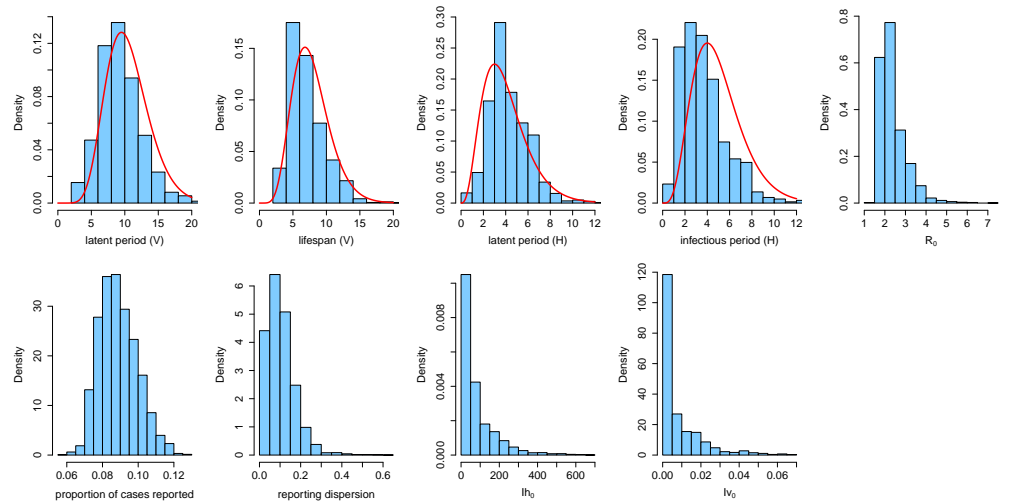

Figure S5. Posterior estimates for Tuamotu-Gambier.
Plot shows marginal posterior estimates for: the mean vector latent period and lifespan; the mean human latent and infectious periods; the basic reproduction number, R_0; the proportion of cases reported, r; the magnitude of environmental noise, ϕ; the number of initially infectious humans, and the proportion of the mosquito population initially infectious. Red lines show the assumed prior distributions for the latent periods in humans and mosquitoes, infectious period in humans, and mosquito lifespan.
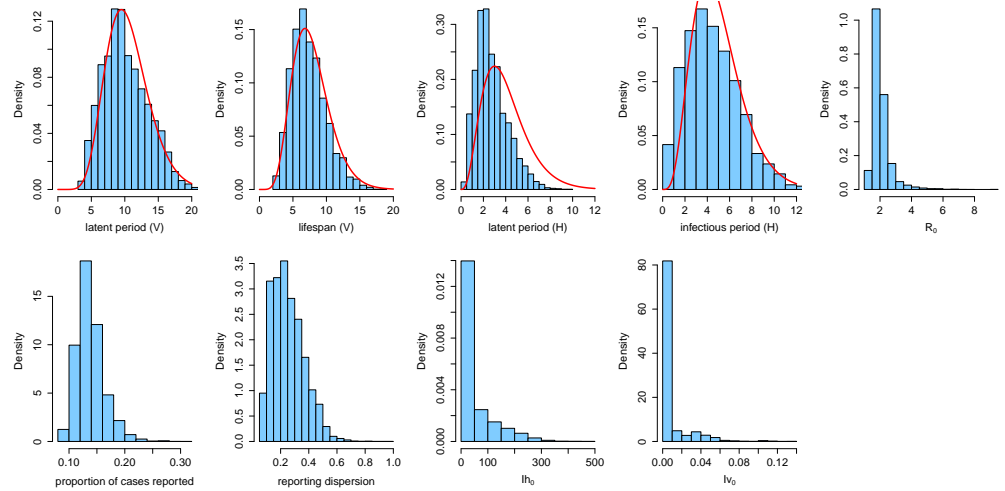
Figure S6. Posterior estimates for Marquises.

Plot shows marginal posterior estimates for: the mean vector latent period and lifespan; the mean human latent and infectious periods; the basic reproduction number, R_0; the proportion of cases reported, r; the magnitude of environmental noise, ϕ; the number of initially infectious humans, and the proportion of the mosquito population initially infectious. Red lines show the assumed prior distributions for the latent periods in humans and mosquitoes, infectious period in humans, and mosquito lifespan.
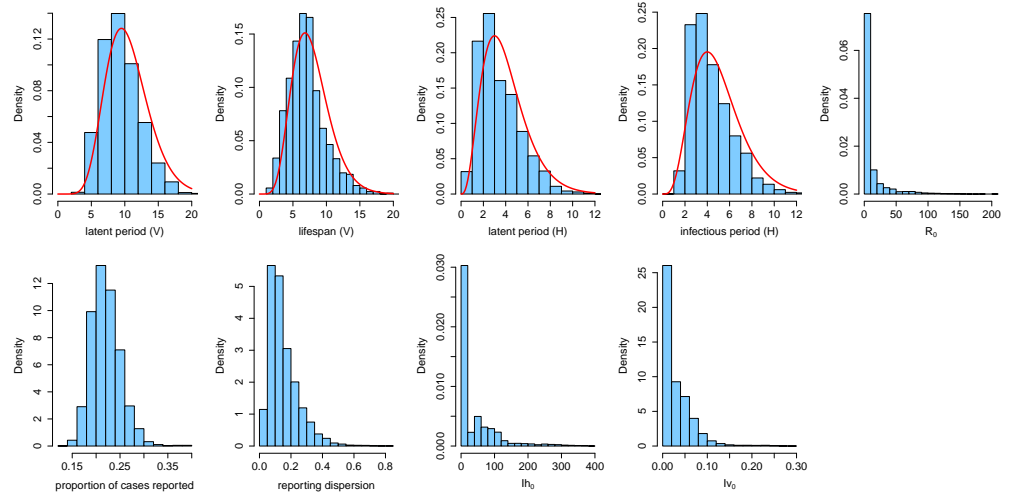

Figure S7. Posterior estimates for Australes.

Plot shows marginal posterior estimates for: the mean vector latent period and lifespan; the mean human latent and infectious periods; the basic reproduction number, R_0; the proportion of cases reported, r; the magnitude of environmental noise, ϕ; the number of initially infectious humans, and the proportion of the mosquito population initially infectious. Red lines show the assumed prior distributions for the latent periods in humans and mosquitoes, infectious period in humans, and mosquito lifespan.